MODELING FREQUENCY DOMAIN EFFECTS

FOR ULTRASONIC FLAW DETECTION

E. R. Green and G. A. Mart

Pacific Northwest Laboratory (PNL)
Operated by Battelle Memorial Institute
Battelle Boulevard
Richland, WA 99352

INTRODUCTION

Experimental studies [1,2] have shown that changing components of an ultrasonic inspection system can greatly affect the amplitude of the echo response from a defect even when conventional calibration procedures [3] are employed. This reduces the reliability of defect detection and sometimes (depending on the sizing method used) defect sizing.

Mathematical models have been developed at PNL for the entire ultrasonic inspection system including the pulser, piezoelectric element, receiver, shoe, and inspection sample. The ultrasonic inspection system model will be used to: 1) perform a more rigorous analysis of equipment interaction than would be possible in experimental studies, and 2) provide a technical basis for current standards [4] for equipment operating tolerances which are presently based on engineering judgement. The model for the electrical equipment have been described previously [5], so this paper will focus on the model for the acoustical portion of the inspection system.

RAY TRACING MODEL DESCRIPTION

A two-dimensional, elastodynamic-physical-optics (EPO) model is used to calculate the transfer function (i.e., frequency domain response) of the acoustical portion of the inspection system as shown in Fig. 1. The transfer function is calculated by calculating the single frequency amplitude and phase response over a range of frequencies. Several simplifying assumptions are made.

- The face of the sending piezoelectric element is assumed to move as a rigid piston. Actually, piezoelectric elements tend to displace more in the center than along the edges, and there are local variations in the piezoelectric material; but the rigid piston assumption seems acceptable since excellent agreement was found

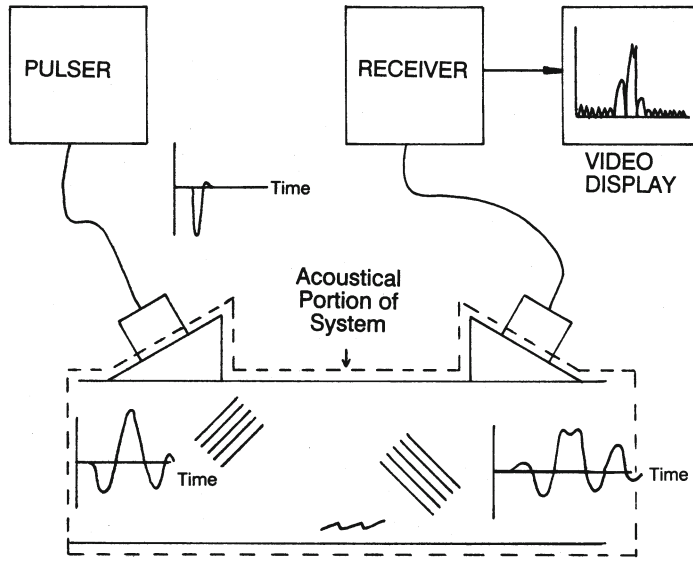

Fig. 1. Generalized ultrasonic inspection system

between calculated beam patterns and those measured from commercially available piezoelectric elements.

- The ultrasonic couplant is assumed to produce no significant reverberation or attenuation. This assumption is justified when the surfaces to be coupled are smooth and match contours within a small fraction of a wavelength and when common fluid couplants (e.g., water, light oil, and ultrasonic gelatin) are used.

- The acoustic media is assumed homogeneous and isotropic.

- The defect is assumed to be a smooth, flat, semi-infinite strip with traction-free faces. This idealized flaw may be thought of as representing a fatigue crack.

- As a first approximation, the face of the receiving piezoelectric element is assumed to be locally reactive.

- EPO theory is a high-frequency approximation that is considered valid for defect sizes greater than a few wavelengths. EPO theory does not take into account diffraction and surface-wave mode conversion effects. A more detailed discussion of the validity of the EPO theory is given by Chapman [6].

The model combines ray tracing and the principal of superposition in the following algorithm. The calculations are coded in FORTRAN 77 and performed on a VAX 11/780 computer.

(1) The sound path of interest (e.g., a traverse wave incident on the defect with mode conversion to a longitudinal wave) is specified.

(2) The surface of the sending piezoelectric element (represented in the 2-D model as a line) is divided into small segments.

(3) A fan of rays from the center of a segment is considered. The initial amplitude of a ray is arbitrarily taken to be 1.0. Based

on the initial angle of a ray, the initial amplitude and phase of the ray is modified by the function given by Miller and Pursey [7] or Roderick [8] for the directivity of a surface-normal point-force source. A ray is traced as it travels through the shoe, refracts into the sample, reflects within the sample, refracts into the receiving shoe, and intersects the receiving piezoelectric element face according to the path specified in step (1). The reflection coefficients are taken from Graff [9], and the refraction coefficients are from Kuhn and Lutsch [10]. By reciprocity, the Miller and Pursey function is applied to a ray at the receiving piezoelectric element face. During its journey, the amplitude of a ray is decreased by a factor of $1/\sqrt{r}$ in accordance with cylindrical spreading (2-D model); and when mode conversion occurs, the radius of curvature is correspondingly modified. The phase of a ray corresponding to each of the discrete frequencies of interest is calculated based on the distance traveled and the phase of the refraction and reflection coefficients. The end result of this step is the pressure (amplitude and phase) in the fluid couplant between the receiving piezoelectric element and its shoe due to a single sending piezoelectric element segment. This pressure is known at the irregularly spaced locations produced by the intersection of the fan of rays with the surface.

(4) Linear interpolation is used to estimate the single-element pressure field along the receiving piezoelectric element face at regular intervals.

(5) Steps (3) and (4) are repeated for all of the sending piezoelectric element segments, and by superposition, the results are added vectorially to obtain the pressure field acting on the receiving piezoelectric element.

(6) The pressure field is integrated numerically over the piezoelectric element face to obtain the acoustical system input to the piezoelectric element which has been assumed to be locally reactive. The result is the acoustical system response (amplitude and phase versus frequency) associated with the specified sound path.

(7) Steps (1) through (6) are repeated for all reasonable sound paths, and the responses are added vectorially to obtain the transfer function for the acoustical system. The temporal response can be found by convolving the system transfer function with the input waveform frequency spectrum and taking the inverse Fourier transform as was done by Chapman and Toft [11]

By dividing the piezoelectric element face into elements and adding the responses of all of the elements by superposition, the need to specify the piezoelectric element beam pattern has been eliminated.

MODEL VALIDATION

Model predictions were compared with experimental measurements to establish the validity of the model for specular reflection from smooth, flat, traction-free defects. Two types of experiments were performed: 1) single-frequency beam-pattern measurements and 2) ultrasonic spectroscopy measurements.

The single-frequency beam-pattern measurements consisted of 90°-corner, pulse-echo measurements; through-transmission, pitch-catch measurements; and tandem search unit configuration measurements. Figure 2

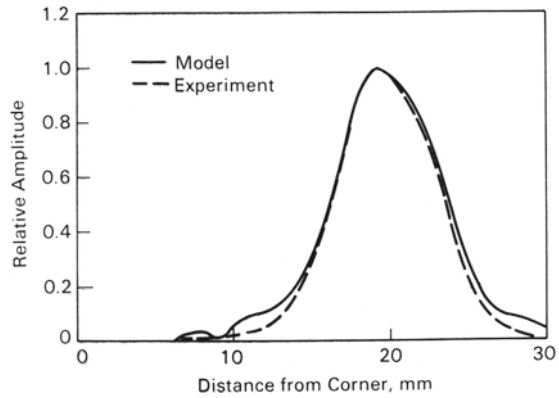

Fig. 2. 90° corner reflection measurement for 20-mm-thick steel at 5 MHz

shows the results of a comparison for a 90°-corner measurement. The echo amplitude from a 13-mm diameter, 5-MHz, 45°-SV (vertically polarized shear) search unit (piezoelectric element plus shoe) used in a pulse-echo configuration is plotted as a function of distance from the corner. Agreement between the model and experiment is excellent. Similar comparisons were made for 45° longitudinal-wave, through-transmission at 1 MHz and tandem search unit scans of smooth strip flaws at 2.25 MHz; and again, the agreement between theory and experiment was excellent. Comparisons for tandem search unit scans of circular-shaped flaws (flat-bottomed holes) showed poor agreement between theory and experiment. The lack of agreement for circular flaws is not surprising given that the model is two-dimensional. It is concluded that the model is valid for single-frequency specular reflection from smooth strip flaws. The model is not valid for circular-shaped flaws.

A set of experiments was performed to test the validity of the model for predicting the frequency dependence of the specular reflection from a smooth flat flaw. As shown in Fig. 3, a 45°-SV, broadband, pulse-echo-configuration search unit was used in a study of

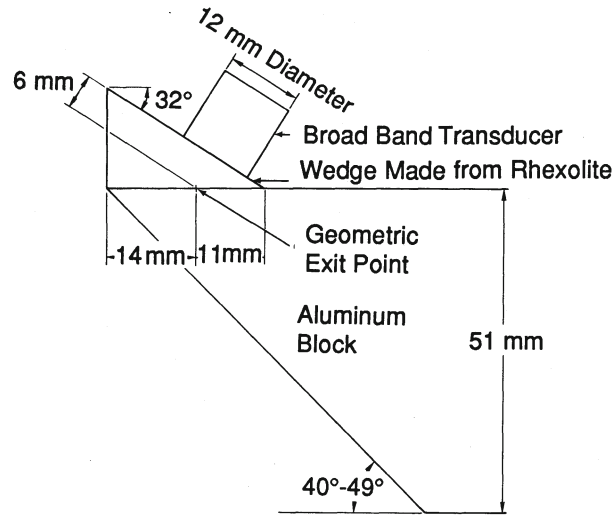

Fig. 3. Configuration used for transfer function versus angle study

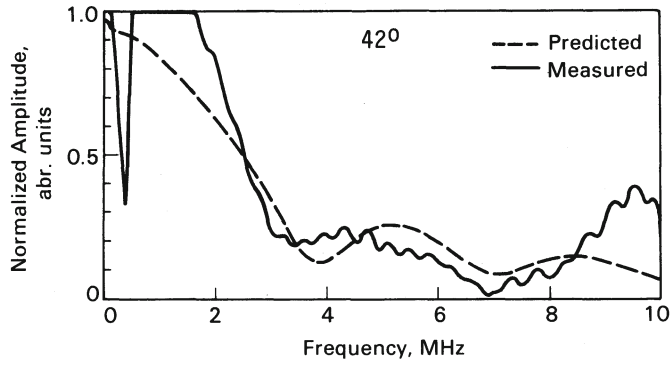

Fig. 4. Specular reflection transfer function for 42° aluminum block

specular reflection from the ends of aluminum blocks with end angles of 40° through 49°. A personal-computer-based ultrasonic-spectroscopy system adapted from the ultrasonic field measurement system of Good et al. [12] was used to trigger the square-wave pulser and to record the echo response. In Fig. 4, measured and calculated transfer functions for the 42° block end are plotted. The level of agreement between theory and experiment shown is typical of that found at the other angles. Both of the curves were normalized by dividing by the transfer function of a 45° block end (the transfer function of a 45° block end is essentially a flat line). The range of validity of the experimental data is 700 kHz to 6 MHz as limited by the bandwidth of the electronic equipment (primarily the search unit). The model does a good job of predicting the shape of transfer function, and the quantitative agreement is generally good. The differences between the theory and the measurements are most likely due to 1) small differences in beam angle between the modeled system and the actual system, coupled with the relatively large transfer function changes that occur with a 1° angle change; 2) the model assumption of a locally reactive receiving piezoelectric element; and 3) the sensitivity of the system to operational parameters not accounted for in the model, like couplant viscosity and search unit skew. The conclusion is that for smooth, flat strip flaws, the model is able to predict transfer functions associated with specular reflection with acceptable accuracy.

MODEL RESULTS

The ray tracing model was used to calculate transfer functions for the acoustical portion of the typical ultrasonic inservice inspection system shown in Fig. 5. In this study, only three variables were investigated; namely, search unit position, defect size, and defect angle. In each case, the curve has been normalized by dividing by the calculated signal frequency amplitude (2.25 MHz) for a 10% through-wall vertical (angle in Fig. 5 of 90°) notch. Unless stated otherwise, the search unit may be assumed to be at the maximum response location.

Figure 6 presents calculated transfer functions for vertical defects of various sizes. A curve representing the transfer function of typical electrical equipment (pulser, piezoelectric element, receiver) is also shown for illustrative purposes. For this case (smooth, flat, vertical strip flaws), the amplitude is not strongly frequency

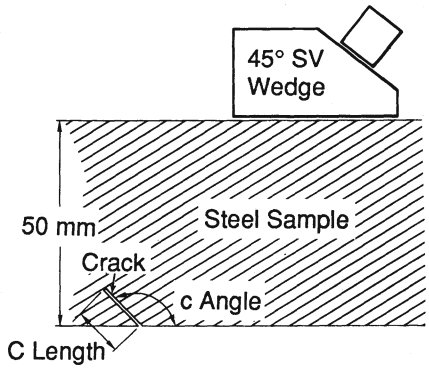

Fig. 5. Pulse-echo ultrasonic test system

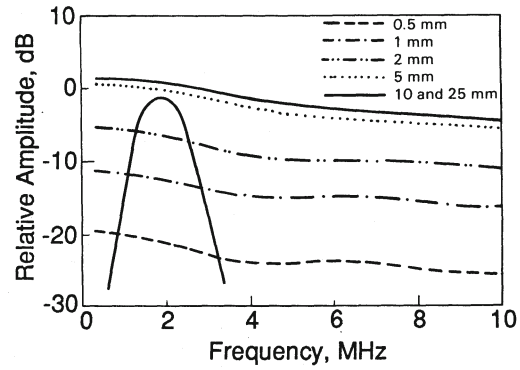

Fig. 6. Frequency response for vertical flaws of various lengths

dependent and is directly proportional to flaw size. The total inspection system response (i.e., the displayed echo amplitude) is a result of the convolution (vector multiplication) of the equipment transfer function and the flaw transfer function; thus, reasonable (e.g., ±25%) changes in equipment bandwidth and center frequency would have almost no effect on the normalized specular-reflection echo amplitude. Similar results were found for 135° flaws. Note that the transfer function of the equipment system may be more sensitive to some equipment changes than others; e.g., if all the equipment is very broadband except the search unit which is narrow band, then the equipment system transfer function will be very sensitive to search unit bandwidth changes but relatively insensitive to receiver bandwidth changes.

Not all flaw transfer functions are flat like those for the vertical flaws considered above. Figure 7 shows transfer functions for different sizes of flaws oriented at 85°. The transfer functions for the larger flaws decline rapidly with increasing frequency and display minima near typical inspection frequencies such as 2.25 MHz. In sharp contrast to the case of vertical flaws, the calibrated echo amplitude from the larger 85° flaws would change significantly with changes in equipment bandwidth and center frequency. Thus, the model provides an explanation for the previously unexplained variation in echo amplitude with equipment changes found in reference [1]. The model predictions for the 85° flaws also show no obvious relationship between flaw size and specular reflection amplitude.

Search unit position also effects the flaw transfer function as shown in Fig. 8. The maximum amplitude search unit position in this case is 52 mm. As the search unit position deviates from 52 mm, the transfer function slope becomes more negative and minima develop, making the calibrated echo amplitude more sensitive to equipment changes. The main point to be made here is that defect sizing methods that rely on echo amplitude as a function of search unit position are also sensitive to inspection equipment changes.

In summary, the model predicts that in general the transfer functions for flat, smooth strip flaws are complicated functions of frequency. The transfer function may have minima which in many cases are located near typical inspection frequencies causing the calibrated echo amplitude to be very sensitive to inspection equipment bandwidth and center frequency. The shape of the transfer function and the positions

of the minima are due to defect size, defect orientation, search unit position, and search unit size.

OBSERVATION

It would be of great benefit to eliminate the transfer function minima, as this would greatly decrease the sensitivity to equipment operating parameters such as bandwidth and center frequency. Removing the minima might also make possible simple relationships between flaw size and signal amplitude, thus adding additional information for flaw sizing. Presently, echo amplitude does not provide useful sizing information.

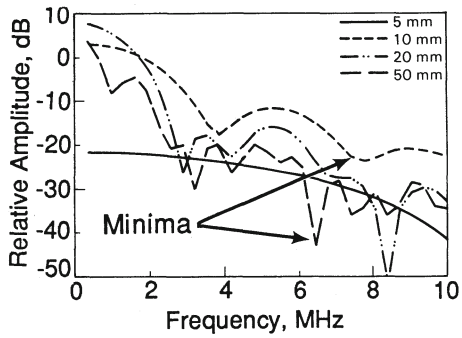

Fig. 7. Frequency response of various sizes of 85° flaws

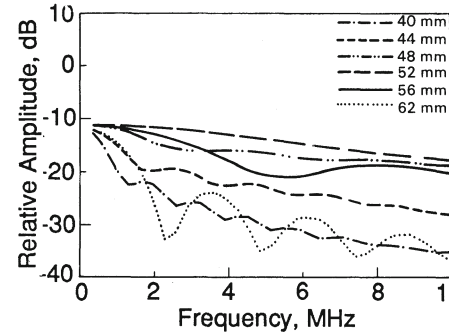

Fig. 8. Frequency responses for 1-mm, vertical flaws for various probe positions

An investigation was made to find out why the predicted flaw transfer functions have minima. It was found that the minima occur due to phase differences in the sound incident on the receiving piezoelectric element. In other words, a response minimum occurs when the returning wavefront is not parallel to the piezoelectric element face so that half the face is in tension and half in compression.

The ideal solution is to use a phase-insensitive receiving piezoelectric element such as a miniature hydrophone receiver, zinc oxide, or cadmium sulphide devices. Such devices unfortunately are not, in general, commercially available. At PNL, an L-wave microprobe developed in our laboratory is used as a phase-insensitive piezoelectric element [12]. The practical solution for most users is to use dual element and tandem configuration search units with a receiving piezoelectric element that is as small as practical given the necessary cable lengths and receiver input impedance.

The argument given above for using a small receiving piezoelectric element does not carry over to the sending piezoelectric element. Factors such as the length of the near field and the desired volume of insonification should dictate the size of the sending piezoelectric element.

SUMMARY AND CONCLUSIONS

- A two-dimensional elastodynamic-physical-optics (EPO) model for calculating the transfer function of the acoustical portion of an ultrasonic inspection system has been proven effective in evaluating system performance through comparisons with single-frequency, beam-pattern measurements and ultrasonic spectroscopy measurements.

- The model predicts that, except for certain cases, the transfer functions for flat, smooth flaws are complicated functions of frequency. The transfer function may have minima which in many cases are located near typical inspection frequencies causing the echo amplitude to be sensitive to inspection equipment bandwidth and center frequency, thus reducing inspection reliability.

- It is suggested that the receiving piezoelectric element for dual element search units and tandem configuration search units be made as small as practical to reduce the sensitivity to equipment changes.

ACKNOWLEDGEMENT

Work supported by the U.S. Nuclear Regulatory Commission under Contract DE-AC06-76RLO 1830; NRC FIN No. B2289; Dr. J. Muscara, NRC Program Monitor.

REFERENCES

1. F. L. Becker, S. R. Doctor, P. G. Heasler, C. J. Morris, S. G. Pitman, G. P. Selby, and F. A. Simonen, NUREG/CR-1696, PNL-3469, Vol. 1, pp. 111-170, 1981. Available from GPO Sales Program, Division of Technical Information and Document Control, U.S. Nuclear Regulatory Commission, Washington, D.C. 20555.
2. D. E. MacDonald and S. M. Walker, EPRI Report No. NP-5485 Research Project 1570-2, 1987. Available from Research Reports Center, Box 50490, Palo Alto, CA 94305.
3. ASME Section XI, Appendix III.
4. ASME Code Case N-409, Revision 1.
5. G. A. Mart and S. R. Doctor, in Proceedings 8th International Conference on NDE in the Nuclear Industry, Orlando, FL, November 17-20, 1986, pp. 325-331.
6. R. K. Chapman, NDT Applications Centre, CEGB, Wythenshaw, Manchester, United Kingdom, CEGB Report No. NWR/SSD/84/0059/R, PWR/RRC/MWG/P(84)378, 1984.
7. G. F. Miller and H. Pursey, in Proceedings of the Royal Society, A223, 1953, pp. 521-541.
8. R. L. Roderick, "The Radiation Pattern from a Rotationally Symmetric Stress Source on a Semi-Infinite Solid," Metals Research Lab, Brown University (date unknown).
9. K. F. Graff, Wave Motions in Elastic Solids, Ohio State Unversity Press, 1975, pp. 311-321.
10. G. J. Kuhn and A. Lutsch, JASA, Vol. 33, No. 7, July 1961, pp. 949-954.
11. R. K. Chapman and M. W. Toft, in Proceedings, 4th European Conference on NDT, London, September 1987, NDT Applications Centre, CEGB, Wythenshawe, Manchester, United Kingdom.
12. M. S. Good and L. G. Van Fleet, in Review of Progress in Quantitative Nondestructive Evaluation, edited by D. O. Thompson and D. E. Chimenti (Plenum Press, New York, 1988), Vol. 7A, pp. 637-646.